JACS
JOURNAL OF THE AMERICAN CHEMICAL SOCIETY

Communication

pubs.acs.org/JACS

Anomalous Reactivity of Ceric Nitrate in Ruthenium "Blue Dimer"-Catalyzed Water Oxidation

Jamie A. Stull,[†] R. David Britt,[†] Jeanne L. McHale,[‡] Fritz J. Knorr,[‡] Sergei V. Lymar,[§] and James K. Hurst*[,‡]

[†]Department of Chemistry, University of California—Davis, Davis, California 95616, United States

[‡]Department of Chemistry, Washington State University, Pullman, Washington 99164, United States

[§]Chemistry Department, Brookhaven National Laboratory, Upton, New York 11973, United States

Supporting Information

ABSTRACT: At high concentrations, nitrate ion alters the dynamics of ruthenium "blue dimer"-catalyzed water oxidation by Ce(IV) such that the oxidation rate is enhanced and a unique reaction intermediate accumulates. This intermediate is characterized by distinct EPR, optical, and resonance Raman (RR) spectra, with the appearance in the latter of a new oxygen isotope-sensitive band. Both Ce(IV) and nitrate are required to generate this intermediate, which suggests ceric-nitrate complexes as the causative agents. Use of ^{18}O-labeled and ^{15}N-labeled materials has established that (1) the new RR band is not an O−O stretching mode (for example, as might be associated with a peroxo species) but involves the O atom coordinated to a Ru center, and (2) the O_2 product does not contain an O atom derived from nitrate, eliminating several plausible pathways involving O-atom transfer to oxidized dimer. Although these results are surprising, similar phenomena have been reported for water oxidation catalyzed by monomeric Ru complexes. The dramatic effects observed for the "blue dimer" make it an ideal candidate for further study.

As the first documented homogeneous water oxidation catalyst,[1] *cis,cis*-$[(bpy)_2Ru(OH_2)]_2O^{4+}$ has received intense scientific scrutiny.[2,3] A considerable body of evidence suggests that, in most media, this complex undergoes four sequential one-electron oxidations with loss of protons to give an O-bridged diruthenyl complex as the catalytically active form:[4,5] where only

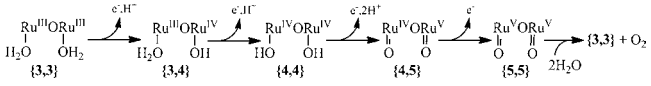

the diruthenyl core of the catalyst is shown and the notation {3,3}, etc., is used to indicate the formal oxidation state on each ruthenium atom. The protonation states shown for {3,3} and {3,4} correspond to weakly acid media; {4,5} is unstable with respect to disproportionation at pH < 2, as is {4,4} at pH > 2.[6] One unusual aspect of "blue dimer" reactivity that has apparently gone unnoticed is that its redox reactions with ceric ammonium nitrate (CAN) differ from other commonly used chemical oxidants, as is evident from the detection of a unique reaction intermediate by chemical dynamics and trapping studies. Data bearing upon this point are discussed below.

As shown in Figure 1, four distinct low-temperature EPR signals have been reported for the "blue dimer" under various

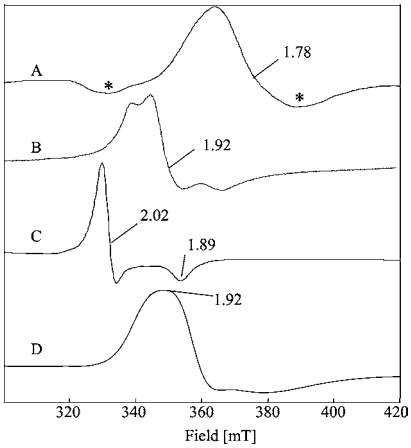

Figure 1. CW EPR spectra of paramagnetic "blue dimer" assigned as (A) {3,4} at pH 9 in borate prepared by oxidation of {3,3} with sodium persulfate (background signals indicated by asterisks on either side of the g = 1.78 signal); (B) {4,5} formed by CPE in 100 mM phosphate, pH 7.2; (C) signal from solutions oxidized to {5,5} by flow-CPE in 0.1 M triflic acid; and (D) an intermediate ({3,4}′) formed by oxidation with CAN in 0.1 M nitric acid. The apparent g-value for spectrum D was taken at the maximum of the derivative CW signal for direct comparison to published EPR spectra.[10]

reaction conditions. The structurally well-defined {3,4} ion formed by one-electron oxidation of {3,3} exhibits a broad rhombic signal in the $g \approx 1.8-1.9$ region of the X-band spectrum whose properties are consistent with an $S = {}^1/_2$ electronic ground state (Figure 1, trace A).[3,7,8] The intensity and position of this signal vary somewhat with pH in acidic solutions, a feature which has been attributed to protonation/deprotonation equilibria involving the coordinated aquo/hydroxo ligands.[7] Two-electron oxidation of {3,4} to {4,5} at pH > 2 generates an $S = {}^1/_2$ species distinguishable by a somewhat higher g-value and lower rhombicity (Figure 1 trace B);[6] below pH 2, this signal rapidly

Received: September 20, 2012
Published: November 26, 2012

   dx.doi.org/10.1021/ja3093532 | J. Am. Chem. Soc. 2012, 134, 19973−19976

disappears with formation of a new relatively narrow axially symmetric signal centered at g = 2.02 (Figure 1, trace C). This latter signal then slowly decays with the reappearance of {3,4} on time scales associated with O_2 evolution.[6,9] This behavior has been rationalized in terms of rapid disproportionation of {4,5} to the EPR-silent {4,4} and catalytically active {5,5} states, with the latter decaying unimolecularly along the catalytic cycle. Appearance of this axial g = 2.02 signal requires four-electron oxidation of {3,3} to {5,5} and can be generated in several ways, including constant potential electrolysis (CPE) in trifluoromethanesulfonic (triflic, HOTf) acid,[7] $Ru(bpy)_3^{2+}$-photosensitzed oxidation by persulfate,[9] and chemical oxidation with Co(III) in nitric or triflic acid or with $Ce(OTf)_4$ in triflic acid (Figure S1).

According to recent data from Pushkar and associates, the axial g = 2.02 signal does not form upon oxidation of the blue dimer by CAN in nitric acid solutions.[10] Instead, a transient with EPR features reminiscent of {4,5} can be trapped by using freeze-quench methods. This species then rapidly decays to give a new broad rhombic EPR signal which is characterized by a g-value at somewhat lower field than the original {3,4} signal. (We have confirmed this behavior, and the latter signal is reproduced as trace D in Figure 1.) XANES analysis suggested that the oxidation state of this species corresponds to Ru^{III}–Ru^{IV}; it was therefore designated as [3,4]′ (herein, {3,4}′).[10] It was also reported that {3,4}′ could be formed upon addition of only two oxidizing equivalents to {3,4}, i.e., did not require prior oxidation to {5,5}, and that decay of {3,4}′ to {3,4} was accompanied by O_2 evolution. In earlier EPR titrimetric studies of {3,3} with CAN in triflic acid, we had also observed {3,4}′,[7] but we did not recognize its significance at that time. Specifically, we found that the axial g = 2.02 signal which formed upon oxidation to {5,5} with a slight excess of CAN declined progressively with increasing addition of CAN in favor of {3,4}′ (Figure S2). During this titration, the nitrate concentration increased from 36 to 144 mM. A wider range of mixing experiments have now revealed a complex relationship between the appearance of {3,4}′ and the nitrate content of the solutions. Addition of $Ce(OTf)_4$ in triflic acid or CAN in nitric acid generate the expected signals at g = 2.02 and 1.92, respectively, which persist in the presence of excess oxidant for at least several minutes. However, when nitric acid is added to $Ce(OTf)_4$-oxidized samples, the g = 2.02 signal rapidly disappears at the expense of the g = 1.92 signal in a dose-dependent manner (Figure 2). Note also the loss of residual {3,4} (g = 1.78), which reflects the continued oxidation of complex by ceric ion. When the order of addition of $Ce(OTf)_4$ and nitric acid is reversed, a different pattern of reactivity is observed which includes titrimetric progression through an EPR-silent state (Figure S3). Similar behavior was reported by Pushkar and co-workers in their freeze-quench experiments with CAN in nitric acid.[10]

Nitrate-dependent features are also found in the RR spectra of the higher oxidation states of the dimer. In 2000, Yamada and Hurst reported that frozen solutions of CAN-oxidized {3,3} in triflic acid exhibited a new oxygen isotope-sensitive band at ~688 cm^{-1}, whose intensity increased progressively with increasing concentrations of CAN at the expense of {5,5} (identified by its ruthenyl Ru═O stretching frequency at ~810 cm^{-1}).[8] These data are reproduced in Figure S4. To account for the concentration-dependent loss of the Ru═O mode and the unusual frequency of the new band, they suggested that it arose from coordination of Ce(IV) to the ruthenyl oxygen atoms to form a 6-membered ring structure. However, recent work indicates that appearance of this band requires nitrate ion. In

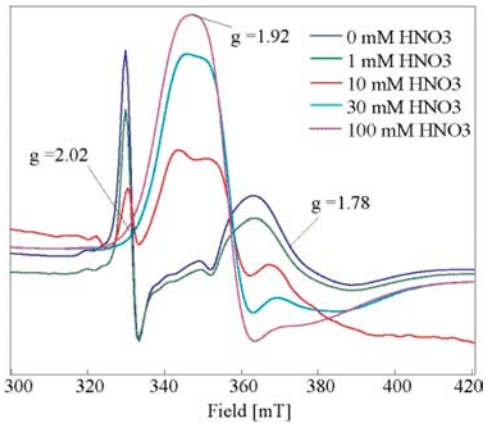

Figure 2. Progressive transformation of the g = 2.02 ({5,5}) and 1.78 ({3,4}) signals to g = 1.92 ({3,4}′) with addition of increasing amounts of HNO_3. The initial solution was prepared by reacting {3,3} (0.9 mM) in 0.1 M triflic acid with ~10-fold excess of ceric triflate.

particular, frozen solutions of $Ce(OTf)_4$ in triflic acid exhibit normal {5,5} RR spectra, that is, from which the 688 cm^{-1} band is absent; addition of nitrate over the concentration range of ~20–140 mM causes progressive conversion of {5,5} to the new species, paralleling the {5,5}→{3,4}′ conversion measured by EPR spectroscopy. The 688 cm^{-1} band has also been observed by Pushkar and co-workers in samples oxidized by CAN in nitric acid.[10] These researchers have proposed that the band is associated with a peroxo intermediate formed via nucleophilic addition of water to an electrophilic ruthenyl oxo atom. Spectra taken in 50% ^{18}O-labeled water indicate that the 688 cm^{-1} band is not an O–O stretching mode, however. Under these conditions, an O–O stretch would give an apparent three-band cluster, i.e., two bands of equal intensity at frequencies corresponding to the ^{18}O–^{18}O (~646 cm^{-1}) and ^{16}O–^{16}O (~688 cm^{-1}) isotopomers with an additional intermediary band at approximately twice the intensity arising from ^{18}O–^{16}O mixed-isotope modes. As seen in Figure 3, only two bands appear in this region. Alternatively, the 688 cm^{-1} band might arise from

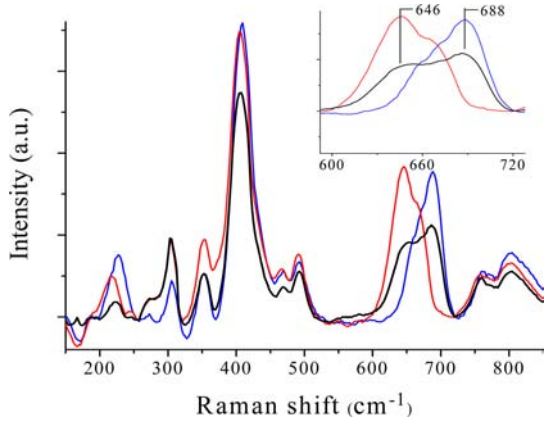

Figure 3. Low-frequency resonance Raman spectra of {3,4}′ in frozen 0.1 M HNO_3 solutions with various ^{18}O-isotopic compositions: normal water (blue line); 92% $H_2{}^{18}O$ (red line); 46% $H_2{}^{18}O$ (black line). Samples were prepared by oxidizing 1–2 mM {3,3} with ~4-fold excess of CAN, then freezing in liquid nitrogen ~1 min after mixing. The inset gives an expanded view of the 600–720 cm^{-1} region, which clearly establishes the absence of an additional band in the 50/50 isotopic composition solution.

dx.doi.org/10.1021/ja3093532 | J. Am. Chem. Soc. 2012, 134, 19973–19976

coupled metal−ligand and intraligand vibrations that contain a strong Ru−O stretching component, as has been suggested by Pushkar and co-workers.[10] Moderately strong out-of-plane deformation modes appear in the Raman spectra of aromatic and nitrogen heterocyclic compounds in this region, including, e.g., the $Ru(bpy)_3^{2+}$ ion.[11] However, this assignment is difficult to reconcile with the magnitude of the measured isotope shift. A putative Ru−^{16}O stretch at 688 cm^{-1} would be down-shifted, at most, to 653 cm^{-1} on ^{18}O substitution, compared to an observed frequency of 646 cm^{-1}. Note, however, that the bands in question are complex: there is a shoulder at about ∼660 cm^{-1} which appears on the red (blue) side of the main peak for the intermediate in $H_2{}^{16}O$ ($H_2{}^{18}O$). It is possible that resonance coupling of similar frequency vibrations on different ligands, as seen for example by Kincaid and co-workers,[12,13] could result in frequency shifts and intensity borrowing, leading to an exaggerated isotope shift and enhancement of the shoulder in the ^{18}O-labeled complex (Figure 3). Alternatively, the 688/646 cm^{-1} bands might be overtones of a lower frequency metal−ligand vibration. We observe a peak at 228 cm^{-1} of the intermediate in normal water which shifts to 217 cm^{-1} in $H_2{}^{18}O$. The first overtones of these vibrations would be obscured by the strong mode at 410 cm^{-1}, but the expected frequencies of the second overtones are in rough accord with the observed peaks at 646 and 688 cm^{-1}. The peak frequencies of the low-frequency (<300 cm^{-1}) bands are subject to uncertainty owing to background subtraction in this range, so further study of this possibility is needed.

It should also be noted that both of the earlier reports on the isotope-dependent RR spectra of this compound[8,10] are ambiguous with respect to the source of the ^{18}O atom. Specifically, spectra taken on complexes with ^{18}O-labeled coordinated water were invariably made in $H_2{}^{18}O$. Thus, upon oxidation to the intermediate, it is unclear whether the heavy O atom was derived from the coordination sphere or the solvent. To resolve this ambiguity, we have repeated these studies using ^{18}O-labeled complex in normal water and vice versa. Upon oxidation with CAN, the isotope-sensitive band for the $H_2{}^{18}O$-coordinated complex in normal water appeared at 650 cm^{-1} and for the inverse labeling pattern, at 694 cm^{-1} (Figure S5). Whatever the source of the band, these data clearly establish that it involves the O atom that was coordinated to Ru in {**3,3**}. Anomalous reactivity of CAN toward a monomeric Ru water oxidation catalyst has been reported by Berlinguette and co-workers.[14,15] These researchers have suggested that this behavior could involve either NO_3^--dependent promotion of specific steps in the catalytic cycle, for example, base-assisted PCET, leading to changes in the rate-limiting step, or direct involvement of $Ce(NO_3)_x^{(4-x)+}$ in the redox cycle, leading to expression of additional reaction pathways, for example, direct O-atom transfer from ceric-bound NO_3^- to a ruthenyl (Ru═O) oxo atom in the oxidized catalyst. The latter possibility is supported by their reported rate law dependence upon CAN and the appearance of NO_2 in the gaseous products of the catalyzed reaction. Similar to these systems, we observe that oxidation of {**3,3**} is markedly accelerated when CAN is used in place of $Ce(OTf)_4$ (S. V. Lymar, unpublished observations). Addition of nitric acid to $Ce(OTf)_4$-oxidized solutions undergoing catalytic turnover also caused immediate changes in the optical spectrum corresponding to complete conversion of {**5,5**} to a species with a unique absorption profile (Figure 4), which is most likely {**3,4**}′. The spectrum of this species slowly changed to {**3,4**} as the reaction progressed. The notion that these effects are a consequence of

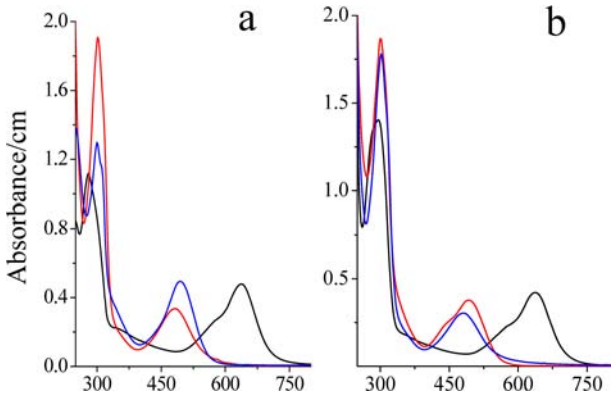

Figure 4. Influence of nitrate upon optical spectra of oxidized blue dimer: (a) 22 μM {**3,3**} in 0.1 M triflic acid (black trace, λ_{max} = 638 nm) oxidized with ∼4-fold excess $Ce(OTf)_4$ (blue trace, λ_{max} = 494 nm), followed by immediate conversion to a unique species (red trace, λ_{max} = 483 nm) upon addition of 0.1 M HNO_3; (b) 19 μM {**3,3**} in 0.1 M HNO_3 oxidized with ∼4-fold excess $Ce(OTf)_4$ with immediate formation of the unique species (blue trace, λ_{max} = 483 nm), followed by slow conversion to {**3,4**} (red trace, λ_{max} = 492 nm). Note the appearance of a shoulder at ∼436 nm, suggesting accumulation of a second intermediate.

base-assisted deprotonation of PCET steps seems improbable, particularly since photochemically driven water oxidation reactions of {**3,3**} made in neutral solutions containing high concentrations of nitrate ion exhibit no unusual properties when compared to solutions containing identical amounts of triflate or perchlorate anions[4] and oxidation by Co(III) is not noticeably accelerated in nitric acid-containing media (J. A. Stull, unpublished observations).

Moreover, with Co(III) as oxidant, {**3,4**}′ did not accumulate under any conditions, including media that contained as much as 0.4 M HNO_3. Instead, EPR, RR and optical features were identical to those observed under other oxidizing conditions. Representative EPR and RR spectra are given in Figures S6 and S7. Thus, both Ce(IV) and nitrate are required for {**3,4**}′ formation. Ceric nitrate complexes are prevalent in nitrate-containing media; using literature data, we estimate that nearly one-half of the total cerium contains ligated nitrate under conditions approximating those used in this study (Figure S8 and its discussion in SI). In contrast, when nitrate is absent, Ce(IV) appears to exist primarily as monomeric and dimeric hydroxo complexes (Figure S8). Coordination may activate nitrate toward oxidation of the catalyst. For example, a recent DFT study of $Ce(OH)(NO_3)_5^{2-}$ finds significant spin density at O atoms of both OH and NO_3 ligands, suggesting that this complex might exhibit radical-like reactivity.[16] The titrimetric behavior wherein nitrate-dependent phenomena emerge only at relatively high nitrate concentrations are also consistent with $Ce(NO_3)_x^{(4-x)+}$ being the oxidant(s) responsible for {**3,4**}′ formation.

Oxidation states of the dimer that are reactive toward $Ce(NO_3)_x^{(4-x)+}$ have not yet been identified. Oxygen atom transfer from ceric-bound NO_3^- to Ru═O[14−16] or addition of coordinated NO_3^- to form a bound peroxynitrate intermediate, are plausible *a priori* mechanisms, given that the ruthenyl center also has considerable oxygen radicaloid character.[5] An illustrative example, which involves dimer cycling between {**3,4**} and {**3,4**}′ coupled to reduction of NO_3^- to HNO_2, is given in Scheme 1.

Reaction by these types of pathways should lead to incorporation of a nitrate oxygen atom into the O_2 product.

dx.doi.org/10.1021/ja3093532 | *J. Am. Chem. Soc.* 2012, 134, 19973−19976

Scheme 1. Hypothetical Pathways for Formation and Decay of Coordinated Peroxynitrate Ion[a]

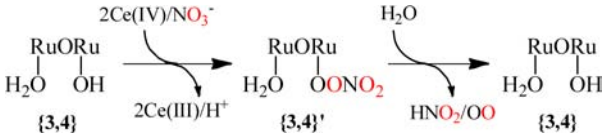

[a]Isotope labeling experiments reported herein exclude these and all other pathways involving O-atom transfer from NO_3^-.

This possibility was probed by adding ~60% ^{18}O-labeled potassium nitrate to a reaction medium comprising $Ce(OTf)_4$ and {3,3} and examining the isotopic composition of accumulated O_2. As shown in Figure 5, none of the ^{18}O was

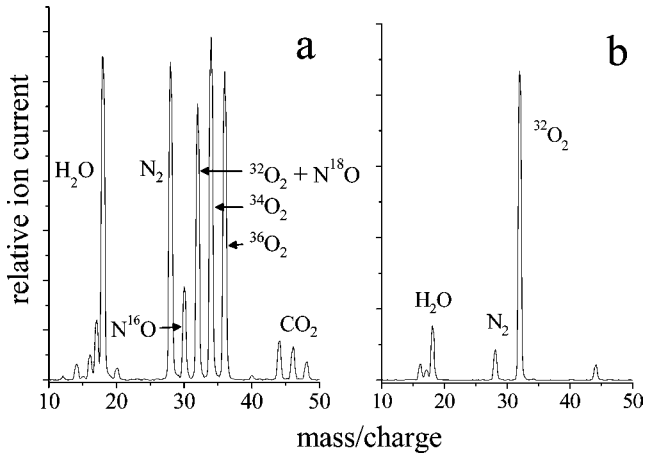

Figure 5. Mass spectra of evolved gases. (a) Thermolysis of ^{18}O-labeled solid KNO_3. The peaks at 44–48 amu are isotopomers of CO_2 introduced as K_2CO_3 impurity (see SI). (b) Reaction of 0.12 mM {3,3} with 5 mM CAN in 0.1 M triflic acid containing 0.12 M 60% ^{18}O-labeled KNO_3. $^{32}O_2$ was also the only oxygen isotope observed when reaction was initiated by adding solid CAN and ^{18}O-labeled KNO_3 to the {3,3} solution.

incorporated into O_2 product; NO and NO_2 resulting from HNO_2 decomposition were also undetectable in the mass spectra of product gases. These observations effectively eliminate from consideration mechanisms that involve O–O bond formation by O-atom transfer from nitrate. Additional EPR studies using ^{15}N-labeled NO_3^- and RR studies using both ^{15}N- and ^{18}O-labeled NO_3^- gave no evidence for incorporation of atoms derived from nitrate into the anomalous reaction intermediate. (Relevant RR and EPR parameters observed for the intermediates under all reaction conditions are compiled in Table S1.)

In summary, these studies clearly demonstrate that ceric coordination activates nitrate ion toward O_2-forming oxidative reactions with the blue dimer. A straightforward interpretation of this effect that involves formation of Ru-peroxo intermediates within the catalytic cycle[4,10] does not survive the experimental scrutiny based on isotope-labeling. Specifically, the RR, EPR, and MS product data indicate that mechanisms involving formations of peroxynitrato and hydroperoxy intermediates do not occur. The alternative possibility that oxidative addition to a bipyridine ligand has occurred can likewise be excluded on the basis of the solvent ^{18}O isotope-dependence of the RR band. However, reactions occurring in the $Ce(IV)/NO_3^-$ environment might modulate the rates of elementary redox steps in the water oxidation cycle, leading to a change in the rate-limiting step with accumulation of a new {3,4}′ intermediate. Given the widespread use of CAN as an oxidant in the study of metal-catalyzed water oxidation[4] and the recent demonstration of nitrate-dependent phenomena involving a mononuclear Ru catalyst,[14,15] it seems likely that forthcoming discoveries on "blue dimer" reactivity will be broadly applicable to other homogeneous water oxidation catalysts.

■ ASSOCIATED CONTENT

Supporting Information

Experimental procedures; additional EPR and RR spectra and a table summarizing these data; detailed description of the mass spectrometric setup. This material is available free of charge via the Internet at http://pubs.acs.org.

■ AUTHOR INFORMATION

Corresponding Author

hurst@wsu.edu

Notes

The authors declare no competing financial interest.

■ ACKNOWLEDGMENTS

This work was funded by the Division of Chemical Sciences, Geosciences, and Biosciences, Office of Basic Energy Sciences, Office of Science, U.S. Department of Energy, through Grants DE-FG02-06ER 15820 (to J.K.H.) and DE-SC00-07203 (to R.D.B.) and (at BNL) by Contract DE-AC02-98CH10886, and by the National Science Foundation through Grant CHE 1149013 (to J.L.M.).

■ REFERENCES

(1) Gilbert, J. A.; Eggleston, D. S.; Murphy, W. R.; Geselowitz, D. A.; Gersten, S. W.; Hodgson, D. J.; Meyer, T. J. *J. Am. Chem. Soc.* **1985**, *107*, 3855–3864.
(2) Lui, F.; Concepcion, J. J.; Jurss, J. W.; Cardolaccia, T.; Templeton, J. L.; Meyer, T. J. *Inorg. Chem.* **2008**, *47*, 1727–1752.
(3) Hurst, J. K.; Cape, J. L.; Clark, A. E.; Das, S.; Qin, C. Y. *Inorg. Chem.* **2008**, *47*, 1753–1764.
(4) Clark, A. E.; Hurst, J. K. *Prog. Inorg. Chem.* **2012**, *57*, 1–54.
(5) Yang, X.; Baik, M.-H. *J. Am. Chem. Soc.* **2006**, *128*, 7476–7485.
(6) Cape, J. L.; Lymar, S. V.; Lightbody, T.; Hurst, J. K. *Inorg. Chem.* **2009**, *48*, 4400–4410.
(7) Lei, Y.; Hurst, J. K. *Inorg. Chem.* **1994**, *33*, 4460–4467.
(8) Yamada, H.; Hurst, J. K. *J. Am. Chem. Soc.* **2000**, *122*, 5303–5311.
(9) Cape, J. L.; Hurst, J. K. *J. Am. Chem. Soc.* **2008**, *130*, 827–829.
(10) Moonshiram, D.; Jurss, J. W.; Concepcion, J. J.; Zakharova, T.; Alperovich, I.; Meyer, T. J.; Pushkar, Y. *J. Am. Chem. Soc.* **2012**, *134*, 4625–4636.
(11) Mallick, P. K.; Danzer, G. D.; Strommen, D. P.; Kincaid, J. R. *J. Phys. Chem.* **1988**, *92*, 5628–5634.
(12) Bruha, A.; Kincaid, J. R. *J. Am. Chem. Soc.* **1988**, *110*, 6006–6014.
(13) Bajdor, K.; Kincaid, J. R.; Nakamoto, K. *J. Am. Chem. Soc.* **1984**, *106*, 7741–7747.
(14) Wasylenko, D. J.; Henderson, M. A.; Ganesammorthy, C.; Koivisto, B. D.; Osthoff, H. G.; Berlinguette, C. P. *J. Am. Chem. Soc.* **2010**, *132*, 16094–16106.
(15) Wasylenko, D. J.; Ganesammorthy, C.; Henderson, M. A.; Berlinguette, C. P. *Inorg. Chem.* **2011**, *50*, 3662–3672.
(16) Yoshida, M.; Masaoka, S.; Abe, J.; Sakai, K. *Chem. Asian J.* **2010**, *5*, 2369–2378.